*Manuscript
Click here to download Manuscript: Paper-REV4-NO marked revision - FIG.docx Click here to view linked References

Mathematical modelling and energy performance assessment of air impingement drying systems for the production of tissue paper

Paolo Di Marco[a], Stefano Frigo[b], Roberto Gabbrielli[c*], Stefano Pecchia[d]

[a] Dipartimento di Ingegneria dell'Energia, dei Sistemi, del Territorio e delle Costruzioni - Università di Pisa, Largo L. Lazzarino, 56126 Pisa (Italy), email: p.dimarco@ing.unipi.t

[b] Dipartimento di Ingegneria dell'Energia, dei Sistemi, del Territorio e delle Costruzioni - Università di Pisa, Largo L. Lazzarino, 56126 Pisa (Italy), email: s.frigo@ing.unipi.it

[c] Dipartimento di Ingegneria Civile e Industriale - Università di Pisa, via Bonanno Pisano, 25/b, 56126 Pisa (Italy), phone: +39-050-2217138 email: r.gabbrielli@ing.unipi.it

[d] Novimpianti Drying Technology, Via del Fanucchi, 17, 55014 Marlia Capannori (LU - Italy) email: s.pecchia@novimpianti.com

* corresponding author

Abstract

In this paper an original and exhaustive mathematical modelling of air impingement drying systems for the production of tissue paper in the Yankee-hoods configurations is reported, which offers the possibility to optimize its energy performance. The model takes into account many detailed operative parameters of the overall drying process with the aim to execute its energy and mass balance and to evaluate its energy performances. The validity of the mathematical model has been assessed by comparison with actual data from an existing tissue paper mill. Finally, the energy performances of two different layouts of the air system have been evaluated and compared. Changing the operative parameters of the drying process, such as air jet temperature and speed and moisture content of the extraction air, it is possible to obtain the same paper production with an

energy saving of about 4.5 %. In average, the layout with two parallel air circuits assure an energy saving of about 1 % with respect to the layout with a single air circuit.

Keywords: Yankee hoods, air impingement, energy assessment, tissue sheet drying, paper drying modelling, energy saving

Nomenclature

b [m]: width of the paper sheet that is wrapped on the Yankee cylinder

c_{pd} [J/kg K]: specific heat of the dry fibre

cp_v [J/kg K]: specific heat of steam

c_{pw} [J/kg K]: specific heat of water

c_{p1} [J/kg K]: specific heat of the impingement air

$\overline{c}_{p1}$ [J/kg K]: specific heat of the moist exhaust air at the temperature averaged between T_2 and T_{ea}

$\overline{c}_{pinl}$ [J/kg K]: specific heat of the air from the mill

d [m]: orifice diameter of the nozzles

D [m^2/s]: diffusion coefficient

dA [m^2]: heat exchange surface of the tissue sheet

d_c [m]: contracted orifice diameter

dm_{ev} [kg/s]: mass flow of vapor that is produced during the drying process in $d\theta$

dm_1 [kg/s]: mass flow of the air impinging the transversal stripe of tissue sheet

dT [K]: infinitesimal temperature variation of the sheet during the drying process

$d\theta$ [rad]: infinitesimal angle of wrap

E [-]: Ackermann correction factor

e [-]: air excess factor for the combustion

F [-]: LMTD correction factor

f [-]: open area fraction of the hood

f_c [-]: vena contracta fraction of the air nozzles

h_n [m]: nozzle-to-sheet distance

h [kJ/kg]: the mass enthalpy of the streams

h_{fg} [J/kg]: latent heat of water at the sheet temperature

h_s [J/kg]: heat of sorption

Le [-]: number of Lewis

LHV [J/kg]: lower heating value of the fuel

LMTD [K]: logarithmic mean temperature difference

$\dot{m}_{cond}$ [kg/s]: mass flow of the steam that condensates inside the Yankee cylinder

MCw: moisture content of the wet-end exhaust gas

MCd: moisture content of the dry-end exhaust gas

m_d [kg/s]: mass flow of the dry fibre

$\dot{m}_{ev}$ [kg/s]: mass flow of the water that is evaporated from the tissue sheet during the drying

$\dot{m}_{fuel}$ [kg/s]: mass flow of the fuel in the burner of the Monosystem configuration

$\dot{m}_{fuel\_d}$ [kg/s]: mass flow of the fuel in the burner of the dry circuit of the Duosystem configuration

$\dot{m}_{fuel\_w}$ [kg/s]: mass flow of the fuel in the burner of the wet circuit of the Duosystem configuration

$\dot{m}_{inl}$ [kg/s]: air mass flow intake from the mill into the hoods in the Monosystem configuration

$\dot{m}_{inl\_d}$ [kg/s]: air mass flow intake from the mill into the dry hood in the Duosystem configuration

$\dot{m}_{inl\_w}$ [kg/s]: air mass flow intake from the mill into the wet hood in the Duosystem configuration

m_w [kg/s]: mass flow of the water within the sheet

$\dot{m}_{wc}$ [kg/s]: water mass flow [kg/s] for the coating

$\dot{m}''_{drying}$ [kg/ m^2 s]: mass flow per unit area of the exhaust moist air at θ

$\dot{m}_{w\_fuel}$ [kg/s]: mass flow of the water that is produced during the fuel combustion in the

Monosystem configuration

$\dot{m}_{w\_fuel\_w}$ [kg/s]: mass flow of the water that is produced during the fuel combustion in the wet circuit of the Duosystem configuration

$\dot{m}_{w\_fuel\_d}$ [kg/s]: mass flow of the water that is produced during the fuel combustion in the dry circuit of the Duosystem configuration

Nu_{imp} [-]: Nusselt number of the heat exchange between the tissue sheet and the impingement air

Nu_L [-]: Nusselt number of the heat exchange between the tissue sheet and the air outside the hoods

p_{tot} [Pa]: total pressure of the impingement air

p_{va} [Pa]: partial pressure of the vapor in the impingement air

p_{vp0} [Pa]: partial pressure of the vapor on the evaporating surface of the sheet

Pr_{imp} [-]: Prandtl number of the heat exchange between the tissue sheet and the impingement air

Pr_L [-]: Prandtl number of the heat exchange between the tissue sheet and the air outside the hoods

$\dot{Q}$ [kW]: thermal power of the air to air heat recuperator

Q_c'' [W]: overall heat that is provided to the tissue sheet by the Yankee cylinder during the drying

$\dot{Q}_{loss}$ [W]: thermal power that is lost due to the thermal exchange between the hoods and the mill environment

q_c'' [W/m^2]: heat flux from the steam in the Yankee cylinder to the tissue sheet

q_a'' [W/m^2]: heat flux from the air impingement to the tissue sheet or from the surrounding air when the sheet is or not under the hoods, respectively

R [m]: radius of the Yankee cylinder

Rt_{tot} [m^2 K/W]: overall heat transfer resistance per unit area between the condensate steam of the Yankee and the tissue sheet

R_v [J/kg K]: gas constant of water vapour

Re_{imp} [-]: Reynolds number of the heat exchange between the tissue sheet and the impingement air

Re_L [-]: Reynolds number of the heat exchange between the tissue sheet and the air outside the hoods

R_{stoich} [-]: mass ratio between air and the fuel at the stoichiometric conditions

S [m^2]: the surface of the recuperator

S_{oh} [m^2]: lateral surface of the cylinder outside the hoods

S_{by} [m^2]: overall surface of the two bases of the Yankee cylinder

T [K]: temperature of the tissue sheet along the wrap angle above the Yankee cylinder

T_{cyl} [K]: temperature of the condensate steam inside the Yankee cylinder

T_{ea} [K]: bulk temperature of the exhaust air downstream the drying process at the outlet of the hoods

T_f [K]: film temperature

T_{mill} [K]: temperature of the ambient air in the tissue mill

T_1 [K]: air impingement temperature

T_2 [K]: exhaust air temperature downstream the jet

T_{lim} [K]: maximum allowable temperature at the inlet of the burner due to its structural strength

T_{lim_w} [K]: maximum allowable temperature at the inlet of the burner of the wet circuit due to its structural strength

T_{lim_d} [K]: maximum allowable temperature at the inlet of the burner of the dry circuit due to its structural strength

Tw: temperature of the wet-end air impingement

Td: temperature of the dry-end air impingement

X [kg water/kg dry air]: moisture ratio

U [W/m^2 K]: overall heat transfer coefficient of the air to air heat recuperator

Vw: velocity of the wet-end air impingement

Vd: velocity of the dry-end air impingement

z_r [kg water/kg fiber]: moisture ratio of the tissue sheet

α_{imp} [W/m^2 K]: convective heat transfer between the tissue sheet and the impingement air

α_{mill} [W/m^2 K]: convective heat transfer between the tissue sheet and the air outside the hoods

α_{by} [W/m^2 K]: heat transfer coefficient between the two bases of the cylinder and the environment within the tissue mill

α_{oh} [W/m^2 K]: heat transfer coefficient between the lateral surface and the environment inside the tissue mill

Δh_{evc} [J/kg]: evaporation heat of the water for the coating

Δh_{evy} [kJ/kg]: condensation heat of the steam inside the Yankee cylinder

θ [rad]: generic wrap angle

ε [-]: contraction coefficient of the flux in the nozzle

ρ_1 [kg/m^3]: mass density of the impingement air

λ_1 [W/m K]: thermal conductivity of the impingement air

φ [-]: relative humidity of the air within the boundary layer above the tissue sheet

1.Introduction

The drying process consists of the moisture removal from wet materials thanks to heat and mass transfer mechanisms [1]. It requires large amount of energy due to the high latent heat of the water that has to evaporate. So, it is essential to study in depth the thermodynamic conditions and plant layout of the drying in order to minimize its energy consumption and its environmental impact. Using different configurations of the drying system, such as fluidized bed dryers, try dryers, dry tunnels, several heat and mass transfer mechanisms can be adopted to assure the water evaporation: hot air jets, microwave, vacuum, infrared, microwave-vacuum, hot air-infrared, thermal contact with high temperature surfaces. In industry the drying is required for many materials, such as fruits, vegetables, meat, sausages, wood, plywood, chemicals, paper. The scientific literature about the studies on the drying processes is very extensive in the energy sector due to their large energy

implications. The most meaningful recent examples that be mentioned are described briefly in the following. In [2] the drying of apple slices on drying tray in a combined microwave-hot air flow dryer is experimentally studied in order to assess the effects of the operative conditions on the drying process and to evaluate its specific energy consumption. In [3] an energy and exergy analysis of industrial fluidized bed paddy drying is presented. Using the balance equations of energy and exergy of the drying chamber, a model for the energy performance assessment is presented and validated using experimental data from two test campaigns. In [4] energy and exergy analyses of native cassava starch drying in a tray drier is reported in order to assess the energy performance of the process. Using the first law of thermodynamics, a simple model is proposed in order to assess the energy performances of the process from the experimental data. In [5] the drying rate curves of the olive stone are experimentally obtained. [6] the drying performances in terms of energy consumptions of a microwave-assisted fluidised bed drying of soybeans are evaluated using a mathematical model that is validated using an experimentally activity. In [7] a mathematical framework, that is validated using experimental data, is developed to estimate the drying performance of a mixed-mode solar dryer with potatoes.

In this paper the drying system of the sheets of tissue paper is considered and its energy performances are analysed. Indeed, the production of tissue paper, that requires the evaporation of large amounts of water, is a very intensive energy process. The average consumption of primary energy per ton of paper produced and per ton of evaporated water is about 5800 MJ (about 1600 kWh) and 4000 MJ (about 1100 kWh), respectively [3]. In modern tissue paper mill the sheet drying is contemporarily assured by the steam heated Yankee cylinder, which is wrapped around by the tissue sheet, and by high temperature and speed air jets from two hoods equipped with steam/oil heated air heaters (this configuration can be found, at present, only in old small mills) or with fuel (mainly natural gas) fired burners.

The Yankee-hood dryer is the crucial section of the paper machine due to its large thermal energy consumption. As a consequence of continuously increasing energy costs, the determination of

operating conditions with the lowest energy consumption is essential in order to design and operate the tissue machine and the air drying system in the most efficient and economical way while ensuring the required paper quality and daily production. Even energy savings of few percentages correspond to large amounts of energy, considering that the annual thermal energy consumption of a middle size tissue mill is about 50 GWh.

The overall energy performances of the sheet drying systems depend on many interdependent process parameters in a very complex way. So, this aspect implies that the assessment of the energy performances both in design and operating phase is a very difficult task. This is generally executed without a structured approach on the basis of a very deep knowledge and practical experience of the operative behaviour of the Yankee-hood drying systems.

In this context, a mathematical model for the reliable assessment of the energy performances of the overall drying system, during design phase and energetic diagnosis in existing tissue mills, can be considered an effective and useful tool for designers and plant managers in order to highlight operating conditions with minimum specific energy consumption.

In the scientific and technical literature, several examples of mathematical models about Yankee-hood drying systems for the assessment of the energy performances of tissue sheet production have been proposed. In particular, in [9] a very comprehensive model, that was successively used as reference by several other authors, is reported. This model considers the Yankee hood configurations that are characterized by the presence of the steam coils for the introduction of thermal power into the air system. This configuration is not suitable to reach high temperature values of the impinging air jet. The modern air hoods for tissue sheet production are characterized by one or two fuel burners in order to reach air temperature up to 700°C. In this case the process of heat and mass transfer between the air and the wet paper sheet requires a particular modelling that is not taken into account in [9]. So, the results cannot be considered completely reliable for high air temperature values.

In [10] mass and energy balances of a Yankee-cylinder with a single hood, i.e. a very simple drying

configuration, are reported. The modelling of the heat and mass transfer of water evaporation is neglected and the heat and mass transfer coefficients are simply defined by the user as input data. The psychrometric Mollier enthalpy-air humidity chart is integrated in the model and the thermodynamic states on the chart of the wet air streams upstream and downstream the hood nozzles are evaluated by the mathematical model. In [11], a mass and energy balance of an existing drying duo parallel system with a black box approach is proposed as diagnosis tool. The measurement of the inlet and outlet streams are used to evaluate the actual fuel consumption of the tissue drying without taking into account the drying mechanism of the sheet. In [12] the same authors proposed an energy model of a drying duo parallel system taking into account also the heat transfer between the air and the sheet and neglecting the mass transfer in the drying process. The heat transfer coefficient is simply calculated starting from a guess value and using a user-defined correction relation.

In [13], two mathematical models, which use some field measurements and make it possible to determine the drying rate of existing hoods for a parallel duo drying system, are reported. These models do not take into account the detailed mechanism of heat and mass transfer during the air jet impingement.

In [14], the energy optimization of the Yankee-hood dryer is executed in order to assess the operative configuration with the minimum consumption of an existing paper mill. The mass and energy balance of each system equipment is combined with a very simple model of the drying process of the tissue sheet.

In the context described above, this paper presents an original and exhaustive mathematical model for the simulation and energy performance assessment of Yankee - hood drying systems for tissue paper production. The limits of the methods, that are present in literature, are overcome by the present model in an original way, as described in the following. The heat and mass transfer mechanisms of the sheet drying are integrated within the mass and energy balance of the overall air system in order to obtain reliable results about the tissue production and its energy consumptions. In

particular, the temperature and moisture content of the tissue sheet during the drying along the wrap angle and the temperature and pressure of each stream of the air system can be evaluated. The model uses the most updated relations for the reliable simulation of the tissue sheet drying and takes into account many characteristics of the system that are essential for the reliability of the performance assessment. Using the results of the model it is possible to obtain the best set of the operative parameters, in order to minimize the specific energy consumption. Hence, the effective use of the model here proposed has meaningful practical implications in terms of tissue mill design and operation from the energy point of view.

In literature many detailed contributions concerning the mathematical modelling of the production of high grammage paper in multi-cylinder configuration are present. This kind of production, where the paper is wrapped on many internally heated cylinders thanks to fabric felt, is largely and deeply investigated. A brief description of the most relevant paper is reported below. In [15] an analytical model based on a system of complex differential equations describing the drying process of the paper during the contact with the wet web/internal heated cylinder is described. In [16] the temperature profile of multi-cylinder dryers along the drying process is calculated and validated with experimental data of a real paper mill using a modelling of the heat exchange between the paper and the cylinders. In [17] a very complex differential mathematical model for unsteady state conditions of the thermal contact between felt, paper and cylinder is proposed and numerically solved. The results of the model are compared with data obtained experimentally using infrared measurements of the surface temperature of the cylinders. In [18] a simple model based on the Mollier chart of the multi-cylinder dryers with closed hoods for the vapor suction and of the heat recovery system is proposed. In [19] a block approach for the assessment of the energy consumption of a multi-cylinder newsprint paper machine using the energy and mass balance equations is presented and validated with experimental test on a full scale tissue mill. In [20] a comprehensive method, that is based on energy load audit and energy flow analysis and energy efficiency estimation, for assessing the energy performance of the dryer section is investigated.

The mathematical models of the multi-cylinder dryers cannot be used for the energy assessment of the tissue paper production because (i) the air system with the impingements in the hoods is not present, (ii) the number of cylinders is higher than one as in the tissue production, (iii) a felt for the adhesion of the paper on the internal steam heated cylinders is used, (iv) the thickness and grammage of the paper is so high that the capillary phenomena cannot be neglected during the drying of the paper sheet.

2. Configuration of the drying air system

The wet paper sheet wraps around the rotating internally steam heated Yankee cylinder. The heat transfer for the drying is assured both by the heated cylinder via conduction and by the hot air impingement jets via convection. The configuration of the drying air system (Figure 1) is composed by two parallel air circuits (duosystem configuration), each of them equipped with a gas fired burner that assures the production of high temperature air. Then, the air is blown towards the two hoods. After the impingement, the exhaust air mixed with the evaporated water from the tissue sheet is sucked from the gap between the Yankee cylinder and the hoods. The humid exhaust air is partially extracted both from the wet-end side and the dry-end side and then conveyed to the recuperator and finally to the atmosphere. The remaining part of the humid exhaust airs from the hoods is recirculated to the burners. In order to fulfil the mass balance of the overall circuit, some make-up air enters the drying system together with the fresh air that is necessary for the combustion process. The make-up air feeds both air loops. The fresh air is preheated within a heat exchanger (hereafter called “recuperator”) using the extracted humid air. Five fans assure the circulation of the air within the wet and dry loops, the feeding of the burners and the extraction of the humid air. The fans for the combustion airs are located downstream the recuperator. This fact implies that some further fresh air can be sucked through the valves S1 and S2 (see Figure 1) in order to limit the temperature of the combustion air and consequently ensure the structural integrity of the burners.

INSERT FIGURE 1

3. Mathematical model of the Yankee cylinder – hood drying system

The mathematical model of the drying air system is divided in some parts starting from the following assumptions:

(i) the temperature and humidity profile within the thickness of the thin sheet is uniform and water is always available on the sheet surface. So, the phenomena of water diffusion, that are typical of the high grammage paper, are neglected;

(ii) along the longitudinal direction of the Yankee cylinder, the humidity profile and temperature are uniform neglecting the effect of small differences of water content on the drying process;

(iii) along the longitudinal direction of the Yankee cylinder, the air jets are supposed to be uniformly distributed so that the heat flux of the air impingement on the tissue sheet can be considered as a continuous function that depends only on the wrap angle, neglecting the reciprocal interaction between adjacent air jets;

(iv) the circumferential heat conduction within the Yankee cylinder is neglected due to its high rotational speed.

3.1 Drying process of the tissue sheet

The drying of the tissue sheet, that is attached to the Yankee cylinder along the wrap angle from the press to the doctor blade (from A to E in Figure 2), is assured by two contributions: from one side the sheet is heated by the internally heated Yankee cylinder (conduction) and from the other by the air jets (convection).

INSERT FIGURE 2

So, the energy balance of an infinitesimal piece of tissue sheet at the generic wrap angle (Figure 3) can be expressed with the following equation:

$$(q_c''+q_a'')bRd\theta = (m_d c_{pd} + m_w c_{pw})dT + \left(h_{fg} + h_s\right)dm_{ev} \qquad \text{(eq.1)}$$

INSERT FIGURE 3

The heat flux from the Yankee can be evaluated with the following equation:

$$q_c'' = \frac{1}{Rt_{tot}}(T_{cyl} - T) \qquad \text{(eq. 2)}$$

Rt_{tot} can be directly inserted in the model or, alternatively, can be calculated as the summation of the single heat transfer resistances, such as the condensate layer on the internal wall, the fouling on the internal wall, the Yankee shell, the spray coating on the external surface of the Yankee, the contact between the Yankee and the tissue sheet [21].

Using the heat of sorption it is possible to take into account that the evaporation of the bound water that is included inside the sheet requires an extra amount of energy besides the latent heat of vaporization for free water. In particular, the following expression [21] can be used for the evaluation of h_s:

$$h_s = 0.10085\, R_v \frac{1-\varphi}{\varphi} z_r^{1.0585} T^2 \qquad \text{(eq.3)}$$

When the tissue sheet is outside the hood, so after the last press and between the outlet of the dry-end hood and the doctor blade (A-B and D-E as Figure 4), q_a'' can be evaluated as follows:

$$q_a'' = \alpha_{mill}(T_{mill} - T) \qquad \text{(eq. 4)}$$

where α [W/m^2 K] can be evaluated as follows assuming the geometrical configuration of a laminar flow above a fixed surface with constant temperature (the sheet temperature is evidently constant in each $d\theta$) [22]:

$$T_{wall} = \text{constant} \qquad Nu_L = 0.664\ \mathrm{Re}_L^{0.5}\,\mathrm{Pr}_L^{0.33} \qquad \mathrm{Pr}_L > 0.5 \qquad \text{(eq. 5)}$$

The thermophysical properties for the calculation of Nu_L, Re_L and Pr_L shall be evaluated at the film temperature that is the average between T_{mill} and T.

When the tissue sheet is under the hoods (B-C and C-D as Figure 2), the heat exchange is due to the high temperature air impingement. The convective heat transfer is strongly influenced by the mass transfer due to the vapor flow diffusing from the tissue sheet to the bulk air flow through the laminar boundary film. Indeed, the air jets assure not only the water evaporation from the tissue sheet but also the heating of vapor to the exhaust temperature from the hoods [21]. So, q_a'' under the hoods shall be evaluated as follows [23]:

$$\mathrm{q_a}'' = \alpha_{\mathrm{imp}} \frac{\mathrm{E}}{\mathrm{e}^{\mathrm{E}} - 1}\left(\mathrm{T_1} - \mathrm{T}\right) \qquad \text{(eq. 6)}$$

where E [-] can be evaluated as follows:

$$\mathrm{E} = \frac{\mathrm{dm_{ev}}}{\mathrm{dA}} \frac{\mathrm{c_{pv}}}{\alpha_{\mathrm{imp}}} \frac{\mathrm{T_2} - \mathrm{T}}{\mathrm{T_1} - \mathrm{T}} \qquad \text{(eq. 7)}$$

where

dA [m^2] can be evaluated as $bRd\theta$

α_{imp} is evaluated modifying the well-known expression of Martin [24]-[29] in order to take into account the effects of the high temperature of the air jets on the heat transfer mechanism:

$$Nu_{imp} = \frac{\left(\frac{f_c}{100}\right)^{0.9505}\left[3.649 - \left(0.03455 + 4.812\ \frac{f_c}{100}\right)\frac{h_n}{d_c}\right]}{1 + 60.47\ \frac{f_c}{100}} \cdot \left[0.90 + \frac{0.10}{1 + 0.05693\left(\frac{T_1 - 273.15}{100}\right)^3}\right] \mathrm{Re}_{imp}^{\ 0.772}\ \mathrm{Pr}_{imp}^{\ 1/3} \qquad \text{(eq. 8)}$$

where

$f_c = f\ \varepsilon$, f is-the ratio between the overall cross section area of the nozzles and the overall internal surface of the hood ε is the contraction coefficient of the flux in the nozzle [28], and $d_c = d\sqrt{\varepsilon}$.

For the calculation of (eq. 8), it is necessary to evaluate the thermophysical properties of the air jet at the film temperature that is the average between T_1 and T. The dimensionless numbers, Nu_{imp} and Re_{imp}, should be calculated using d_c as characteristic length of the heat transfer process. Moreover, the speed of the impinging air is used to calculate Re_{imp}.

The vapor mass flow that is produced in the drying process (dm_{ev}) can be evaluated using the equation of Stefan [30]:

$$dm_{ev} = \frac{\alpha}{\rho_1 c_{p1} Le^{2/3}} \frac{p_{tot}}{R_v T} \ln\left(\frac{p_{tot} - p_{va}}{p_{tot} - p_{vp0}}\right) dA \qquad \text{(eq. 9)}$$

where

$$Le = \frac{\lambda_1}{\rho_1 c_{p1} D}$$

D can be calculated using the following equation (10) [31]:

$$\begin{cases} D = 1.87\,10^{-10}\,\dfrac{T_f^{\;2.072}}{9.872\,10^{-6}\,p_{tot}} & 280\,\mathrm{K} < \mathrm{T_f} < 450\,\mathrm{K} \\ D = 2.75\,10^{-9}\,\dfrac{T_f^{\;1.632}}{9.872\,10^{-6}\,p_{tot}} & 450\,\mathrm{K} < \mathrm{T_f} < 1070\,\mathrm{K} \end{cases} \qquad \text{(eq. 10)}$$

The energy balance of the impingement air can be expressed in the following way:

$$\left(T_1 - T_2\right) dm_1 c_{p1} = q_a'' dA + dm_{ev}\; c_{pv}\left(T_2 - T\right) \qquad \text{(eq. 11)}$$

Combining the equations 6 and 7, it is possible to obtain the explicit dependence of the exhaust air temperature on the impingement and sheet temperature:

$$T_2 = T_1 - \left(T_1 - T_2\right) = T_1 - \frac{\alpha \dfrac{E\,e^E}{e^E - 1}\left(T_1 - T\right)}{\dfrac{dm_1}{dA}\,c_{p1}} \qquad \text{(eq. 12)}$$

The overall energy balance of the Yankee cylinder has to take into account the presence of some thermal losses, due to the heat exchange between the cylinder and the environment air across its bases, where thermal insulation is sometimes mounted and the heat transfer across the lateral surface of the cylinder not covered by the paper sheet (outside of the hoods) due to the injection of the coating cold water solution. So, $\dot{m}_{cond}$ can be evaluated in the following way:

$$Q_c'' + \dot{m}_{wc}\Delta h_{evc} + S_{by}\alpha_{by}\left(T_{cyl} - T_{mill}\right) + S_{oh}\alpha_{oh}\left(T_{cyl} - T_{mill}\right) = \dot{m}_{cond}\Delta h_{evy} \qquad \text{(eq. 13)}$$

where

α_{by} [W/m^2 K] is calculated–using the reference geometry of the rotating disk in a quiescent fluid

[31]) and α_{oh} is calculated using (eq. 5).

Finally, the bulk temperature of the exhaust air downstream the drying process at the outlet of the hoods (streams 2 and 3 in Figure 1 and 2) (T_{ea}) can be evaluated as follows from the energy and mass balances of the mixing streams of drying air and air intake:

$$\dot{m}_{drying} h_2 + \dot{m}_{inl} h_{mill} - \dot{Q}_{loss} = (\dot{m}_{drying} + \dot{m}_{inl}) h_{ea} \qquad \text{(eq. 14)}$$

which can be rewritten as

$$\int_{\theta_0}^{\theta_h} \bar{c}_{p1}(T_2 - T_{ea}) \dot{m}''_{drying} R\, L\, d\theta + \dot{m}_{inl} \bar{c}_{pinl} (T_{mill} - T_{ea}) - \dot{Q}_{loss} = 0 \qquad \text{(eq. 15)}$$

where

$\dot{m}_{inl}$ enters into the hoods from the mill through the gap between the Yankee cylinder and the hoods, because the pressure is slightly lower than the atmospheric value

$\bar{c}_{pinl}$ [J/kg K] is calculated at an average temperature between T_2 and T_{ea}

The mass and energy balance of the drying air system can be examined in Appendix A.

4. Assessment of the energy performances of the drying system of the duosystem configuration with parallel wet–end e dry–end hoods

4.1 Inputs and validation of the simulation model

The model has been implemented and iteratively solved using MATLAB language [32]. Afterwards, it has been tested and calibrated using actual operative data of an existing tissue mill (see Figure 1 for the layout of the air drying system) as reported in Table 1, where also the main inputs of the model are summarized.

It is necessary to explain some specific features of the input data:

- The width of the tissue sheet on the Yankee cylinder is higher than that on the pope reel due to the presence of the trimmed wasted on the Yankee cylinder.
- The tissue sheet is creped (i.e., its grammage changes from the outlet of the Yankee cylinder and the pope) and, consequently, the peripheral speed of the Yankee cylinder is higher than that of the pope.
- For simplicity, the overall heat transfer coefficient between the steam inside the Yankee cylinder and the tissue sheet is directly provided as input of the model.

The most meaningful outputs from the energy point of view are:

- The specific energy consumption is defined as the ratio between the overall thermal power consumption, i.e. the summation of the gross thermal power of the Yankee cylinder and the term $LHV\ \dot{m}_{fuel}$, and the hourly paper production. The specific energy consumption can be evaluated using the hourly mass flow of the evaporated water in place of the paper production.
- The thermal power of the drying unit is the summation of the net thermal power of the Yankee cylinder and the thermal power that is provided to the tissue sheet by the air jets within the hoods.

In Table 2 the existing plant data and the outputs of the model are summarized for the comparison. It is possible to note that the discrepancy between them is always not higher than 5%. This fact confirms the reliability of the simulation model. It is important to note that it is not possible to compare in a reliably way the proposed model with those that are present in literature, because the other models are not completed as the present one.

INSERT TABLE 1

INSERT TABLE 2

4.2 Assessment of the energy performance

After the validation of the model, the dependence of the energy and production performances of the tissue mill on some important operative parameters has been investigated. First of all, the effect of the overall heat transfer coefficient of Yankee cylinder is analysed (Figure 4). This analysis is generally executed by Yankee cylinder manufacturer or by the tissue mill manager in order to better understand and evaluate the cylinder performances. The decrease of the heat transfer coefficient, that could occur due during the operative life due to straw pipes jamming or syphon damaging, induces a strong penalization of the overall drying performance and energy efficiency, since the heat transfer via the Yankee cylinder is generally more efficient than the air impingement one. Consequently, increasing the plant life the latter has to be used more intensively in order to assure the required water evaporation.

Successively, we investigated how to define the best values of the moisture content of the exhaust air at the outlet of the drying hoods (streams 5 and 10 in Figure 1). The moisture contents of these two streams are very important from the operative point of view, because they are directly managed by the tissue plant manager in order to control the paper machine performances. This can be achieved adopting a suitable control on the extraction fan (V3 in Figure 1) and on shutters that are generally located in the extraction streams (streams 5 and 10 in Figure 1). The results of this analysis (Figure 5) showed that the effect of the moisture content of the wet-end exhaust gas on the energy consumption is lower. So, it is better to reduce the moisture content of the wet-end extraction in order to increase the paper production with a lower increase of the energy consumption.

If the moisture content of the extraction air is higher, the mass flow of the dry air is lower and, consequently, also the make-up air flow rate is lower. It is interesting to note that the paper production decreases when the moisture content of the extraction air streams increases, because the evaporation rate is lower using impingement air with higher moisture content, in accordance with the Stefan law. Indeed, if the extraction air has higher moisture content, also the impingement air is moister. It is important to note that it is impossible to decrease the moisture content of the exhaust air streams below a minimum threshold value because the mass flows of the recirculation streams (streams 6 and 11 in Figure 1) tend to zero when the moisture contents become low.

A third analysis we performed concerns the effect of the impingement temperature on the paper mill performance. In the last years, all manufactures of tissue drying systems increased largely the operative temperature of the impingement jets in order to obtain larger sheet velocity and, consequently, the paper production as denoted in Figure 6. This procedure leads to a marked increase in the energy consumption. Passing from 150°C to 550°C, so from conventional steam heat exchangers to sophisticated gas-fired burners, the specific energy consumption increases in the range 10-30% even if the installation of heat recovery steam generators on hood exhaust line can mitigate this energy increase. The increase of the impingement temperature in the wet-end hood is generally more effective than in the dry-end hood in terms of paper production growth and specific energy consumption decrease.

Finally, the effect of the impingement velocity on the energy and production performances has been analysed (Figure 7). In order to increase the production with the lower energy consumption growth, it is more effective to change the impingement velocity of the wet-end side. In fact, in the dry-end hood, the heat exchange is less effective due to the lower moisture content of the tissue sheet and to the larger role of the sorption heat. In general, higher velocities assure higher evaporation rates and, consequently, larger paper production. Using the same geometry of the hoods, this implies higher mass flow of the air jets and, consequently, the increase of the specific energy consumption.

INSERT FIGURE 4

INSERT FIGURE 5

INSERT FIGURE 6

INSERT FIGURE 7

In Table 3, considering for example a daily paper production of 110 t/d, as in the reference case, we report a summary of the simulated results reported in Figure, 5, 6 and 7. Changing the operative parameters, the specific energy consumption can vary from 1685 kWh/t to 1610 kWh/t, with a percentage saving of about 4.5 %, that corresponds to a large amount of energy for a middle size paper mill.

INSERT TABLE 3

5. Performance comparison with the monosystem configuration

Since the reliability of the mathematical model described above has been demonstrated, it is applied to a different layout of the drying system after some modifications that are listed in Appendix A. After that the energy performances have been evaluated with a similar simulation activity described above. The aim of this analysis is to evaluate how the energy performances of the drying process are affected by the layout of the air system. So, we compare this layout with the duosystem configuration.

The layout that has been taken into account is the monosystem configuration (Figure 8), whose peculiarities with respect to the previous configuration are: (i) only one burner is adopted; (ii) there is only one air circuit; (iii) the hot air stream is divided into two streams that are blown towards the tissue sheet within both hoods; (iv) the humid exhaust air from the wet-end hood is partially recirculated to the dry exhaust air stream and partially extracted and conveyed to the atmosphere.

INSERT FIGURE 8

As the characteristics of the wet-end and dry-end hoods are identical, the following inputs for the hoods for the reference case have been adopted:

(i) the air impingement temperature of the wet-end (dry-end) hood is equal to 450°C,

(ii) the air impingement speed of the wet-end (dry-end) hood is equal to 110 m/s,

(iii) the absolute humidity of the exhaust air from the wet-end side is 500 g/kg,

(iv) the air excess for the burner is 25%.

The results of the reference case are reported in Table 4. The higher moisture content of the air jets due to the higher humidity of the extracted air in the dry-end hood implies lower paper production (the drying rate is lower due to the higher moisture content) (by about 3.6%) and lower energy consumption (by about 1.5%) in comparison with the duosystem configuration in accordance with the results reported in Figure 5.

The energy and production performances in function of the overall heat transfer coefficient of the Yankee cylinder, the moisture content of the exhaust air, the temperature and speed of the air impingement have been evaluated and reported in the following Figure 9, 10, 11, 12, respectively. The performance of the monosystem layout depends on the operative parameters in a similar way to that of the duosystem layout with parallel configuration. In particular, in comparison with the duosystem layout:

1. For the monosystem configuration, the influence of the heat transfer coefficient of the Yankee cylinder on the performance is very similar (Figure 9).
2. For the monosystem configuration, the influence of the moisture content of the exhaust air on the performance is larger (Figure 10). It is important to note that the minimum allowable value of the moisture content is about 330 g/kg because lower values imply that the recirculation mass flow (stream 5 of Figure 8) becomes equal to zero due to the high mass flow of the extraction

flow. Further reductions of the moisture content would imply that the exhaust air extraction could occur also from the dry-end hood (the flow of the stream 5 of Figure 8 would be from the outlet of the dry-end hood to that of the wet-end hood). This operative condition is not usually adopted due to the low energy efficiency.

3. For the monosystem configuration the influence of the impingement temperature is much higher than in the duosystem configuration (Figure 11).
4. For the monosystem configuration the influence of the impingement speed is much higher than in the duosystem configuration (Figure 12).

Comparing the performances of both configurations that we analysed, we can conclude that, using similar operative parameters, the monosystem configuration is characterized by lower energy consumption and lower paper production. If the comparison is executed with the same daily paper production (see Figure 13, where the results of all simulations are summarized in a single view), in the duosystem layout, thanks to its larger number of controllable operative parameters, it is generally possible to find a particular operative setting which corresponds to a lower specific energy consumption than in the monosystem. Finally, it is possible to assess that, if the daily paper production increases thanks to an appropriate modification of the thermodynamic characteristics of the air jets and of the extracted air, the specific energy consumption of the monosystem configuration tends necessarily to increase.

INSERT TABLE 4

INSERT FIGURE 9

INSERT FIGURE 10

INSERT FIGURE 11

INSERT FIGURE 12

INSERT FIGURE 13

Conclusions and future developments

This paper presents an original and exhaustive mathematical model of the drying process in tissue paper production in order to assess its energy consumption and paper productivity as a function of the most important geometrical data and operative parameters of the drying system.

The results of the simulation model differ not higher than 5% from the experimental data of an existing paper mill, assuring its validity as effective tool for the assessment of the energy performances. Then, the model has been applied to two configurations of drying air systems in order to evaluate the dependence of the energy performances on the most meaningful operative parameters.

Keeping the paper production of the reference case, in the duosystem configuration it is possible to reduce the specific energy consumption by about 4.5% changing the operative parameters in their allowable range. Considering the typical energy consumptions of a middle size tissue mill, this value of energy saving corresponds to large amount of energy. The most interesting results with general validity for both layouts that have been considered are: (i) keeping the same paper production, the lowest energy consumptions of a tissue mill can be obtained when (a) a Yankee cylinder with higher heat transfer coefficient is used, (b) the moisture content in the exhaust air is high, (c) the jet temperature and speed are low; (ii) on the contrary, in order to maximize the paper production it is necessary to have (a) high efficient Yankee cylinder, (b) exhaust air with low moisture content and (c) air jets with high temperature and speed.

Considering the same paper production, the plant layout with duosystem configuration is characterized in average by lower energy consumptions with respect to the monosystem layout by about 1%.

The present model could be improved removing some simplifications that have been adopted. In

particular, the interaction of adjacent air jets could be considered for configurations with very narrow holes. Moreover, in some existing old paper machines, the gap between the Yankee cylinder and the hoods can largely vary along the wrap angle and the transversal direction due to construction imperfections. This feature should be considered in order to better estimate the heat and mass transfer coefficient in the impingement process.

The model that has been here proposed can be effectively applied after some modifications to other different layouts of drying systems in order to find less energy-intensive configurations. For example, it may be used for the analysis of a new plant layout that is becoming common in the last years, characterized by a gas turbine whose exhaust gas replaces the gas fired burner, obtaining a combined heat and power configuration.

Appendix A Mass and energy balance of the drying air system

Using the references of the streams as reported in Figures 1 and 8, the mass and energy balance of the drying air system can be expressed in the following way:

- *Duosystem configuration (Figure 1) (the pedices w and d refer to the wet-end and dry-end hoods, respectively)*

Mass balance of the air for the wet-end hood

$$\dot{m}_7 + \dot{m}_{inl\_w} + \dot{m}_{fuel\_w} + \dot{m}_{ev\_w} = \dot{m}_5 \qquad \text{(eq. A1)}$$

Mass balance of the air for the dry-end hood

$$\dot{m}_{12} + \dot{m}_{inl\_d} + \dot{m}_{fuel\_d} + \dot{m}_{ev\_d} = \dot{m}_{10} \qquad \text{(eq. A1bis)}$$

Mass balance of the water for the wet-end hood

$$\dot{m}_7 \frac{X_7}{1+X_7} + \dot{m}_{inl\_w} \frac{X_{inl}}{1+X_{inl}} + \dot{m}_{ev\_w} + \dot{m}_{w\_fuel\_w} = \dot{m}_5 \frac{X_5}{1+X_5} \qquad \text{(eq. A2)}$$

Mass balance of the water for the dry-end hood

$$\dot{m}_{12}\frac{X_{12}}{1+X_{12}}+\dot{m}_{inl\_d}\frac{X_{inl}}{1+X_{inl}}+\dot{m}_{ev\_d}+\dot{m}_{w\_fuel\_d}=\dot{m}_{10}\frac{X_{10}}{1+X_{10}} \qquad \text{(eq. A2bis)}$$

Note that X_5 and X_{10} are inputs of the model as required by the operation of the tissue paper mill.

Mass balance of the burner for the air circuit of the wet-end hood

$$\dot{m}_{20}=R_{stoich}(1+e_w)\dot{m}_{fuel\_w} \qquad \text{(eq. A3)}$$

Mass balance of the burner for the air circuit of the dry-end hood

$$\dot{m}_{24}=R_{stoich}(1+e_d)\dot{m}_{fuel\_d} \qquad \text{(eq. A3bis)}$$

Energy balance of the air to air heat recovery

$$\dot{m}_{17}(h_{17}-h_{25})=\dot{m}_{16}(h_{15}-h_{16}) \qquad \text{(eq. A4)}$$

where the streams 21, 15 and 18 exit the recuperator at the same temperature, because the air flux is split at the outlet of the recuperator

Thermal performance of the air to air heat recovery

$$\dot{Q}=\dot{m}_{17}(h_{17}-h_{25})=U\ LMTD\ SF \qquad \text{(eq. A5)}$$

Energy balance of the fuel fired burner for the air circuit of the wet-end hood

$$\dot{m}_9h_9+\dot{m}_{20}h_{20}+\dot{m}_{fuel\_w}h_{fuel\_w}+LHV\ \dot{m}_{fuel\_w}=\dot{m}_1h_1 \qquad \text{(eq. A6)}$$

Energy balance of the fuel fired burner for the air circuit of the dry-end hood

$$\dot{m}_{14}h_{14}+\dot{m}_{24}h_{24}+\dot{m}_{fuel\_d}h_{fuel\_d}+LHV\ \dot{m}_{fuel\_d}=\dot{m}_4h_4 \qquad \text{(eq. A6bis)}$$

Energy balance of the mixer D

$$\dot{m}_7h_7+\dot{m}_6h_6=\dot{m}_8h_8 \qquad \text{(eq. A7)}$$

Energy balance of the mixer F

$$\dot{m}_{11}h_{11}+\dot{m}_{12}h_{12}=\dot{m}_{13}h_{13} \qquad \text{(eq. A7bis)}$$

Energy balance of the mixer A

$$\dot{m}_{10}h_{10}+\dot{m}_5h_5=\dot{m}_{17}h_{17} \qquad \text{(eq. A8)}$$

Mass balance of the splitter B

$$\dot{m}_{15} = \dot{m}_{12} + \dot{m}_7 \quad \text{(eq. A9)}$$

Mass balance of the splitter C

$$\dot{m}_2 = \dot{m}_5 + \dot{m}_6 \quad \text{(eq. A10)}$$

Mass balance of the splitter E

$$\dot{m}_3 = \dot{m}_{10} + \dot{m}_{11} \quad \text{(eq. A11)}$$

Mass balance of the mixer H

$$\dot{m}_{18} + \dot{m}_{27} = \dot{m}_{19} \quad \text{(eq. A12)}$$

Energy balance of the mixer H

$$\dot{m}_{18} h_{18} + \dot{m}_{27} h_{27} = \dot{m}_{19} h_{19} \quad \text{(eq. A13)}$$

$$\dot{m}_{27} = 0 \text{ if } T_{20} \leq T_{lim\_w} \quad \text{(eq. A14)}$$

Mass balance of the mixer G

$$\dot{m}_{21} + \dot{m}_{23} = \dot{m}_{22} \quad \text{(eq. A15)}$$

Energy balance of the mixer G

$$\dot{m}_{21} h_{21} + \dot{m}_{23} h_{23} = \dot{m}_{22} h_{22} \quad \text{(eq. A17)}$$

$$\dot{m}_{23} = 0 \text{ if } T_{24} \leq T_{lim\_w} \quad \text{(eq. A18)}$$

- Monosystem configuration (Figure 8)

Mass balance of the air

$$\dot{m}_{12} + \dot{m}_{inl} + \dot{m}_{fuel} + \dot{m}_{ev} = \dot{m}_6 \quad \text{(eq. A19)}$$

Mass balance of the water

$$\dot{m}_{12} \frac{X_{12}}{1 + X_{12}} + \dot{m}_{inl} \frac{X_{inl}}{1 + X_{inl}} + \dot{m}_{ev} + \dot{m}_{w\_fuel} = \dot{m}_6 \frac{X_6}{1 + X_6} \quad \text{(eq. A20)}$$

Note that X_6 is an input of the model, because it is established by the plant manager during the

operation of the tissue paper mill.

Mass balance of the burner

$$\dot{m}_{16} = R_{stoich}(1+e)\dot{m}_{fuel} \qquad \text{(eq. A21)}$$

R_{stoich} evidently depends on the type of fuel and e is an input parameter that is selected in order to assure the complete combustion of the fuel respecting the emission limits about the pollutant.

Energy balance of the air to air heat recovery

$$\dot{m}_6(h_6 - h_{17}) = \dot{m}_{12}(h_8 - h_{12}) \qquad \text{(eq. A22)}$$

Note that the streams 8 and 13 are split downstream the recuperator.

Thermal performance of the air to air heat recovery

$$\dot{Q} = \dot{m}_6(h_6 - h_{17}) = U\ LMTD\ S\ F \qquad \text{(eq. A23)}$$

Energy balance of the fuel fired burner

$$\dot{m}_{10}h_{10} + \dot{m}_{16}h_{16} + \dot{m}_{fuel}h_{fuel} + LHV\ \dot{m}_{fuel} = \dot{m}_{11}h_{11} \qquad \text{(eq. A24)}$$

Mass balance of the mixer C

$$\dot{m}_8 + \dot{m}_7 = \dot{m}_9 \qquad \text{(eq. A25)}$$

Energy balance of the mixer C

$$\dot{m}_7 h_7 + \dot{m}_8 h_8 = \dot{m}_9 h_9 \qquad \text{(eq. A26)}$$

Mass balance of the mixer B

$$\dot{m}_5 + \dot{m}_3 = \dot{m}_7 \qquad \text{(eq. A27)}$$

Energy balance of the mixer B

$$\dot{m}_5 h_5 + \dot{m}_3 h_3 = \dot{m}_7 h_7 \qquad \text{(eq. A28)}$$

Mass balance of the splitter A

$$\dot{m}_2 = \dot{m}_5 + \dot{m}_6 \qquad \text{(eq. A29)}$$

Mass balance of the splitter E

$$\dot{m}_{11} = \dot{m}_4 + \dot{m}_1 \qquad \text{(eq. A30)}$$

Mass balance of the mixer D

$$\dot{m}_{13} + \dot{m}_{14} = \dot{m}_{15} \qquad \text{(eq. A31)}$$

Energy balance of the mixer D

$$\dot{m}_{13} h_{13} + \dot{m}_{14} h_{14} = \dot{m}_{15} h_{15} \qquad \text{(eq. A32)}$$

$$\dot{m}_{14} = 0 \text{ if } T_{16} \leq T_{lim} \qquad \text{(eq. A33)}$$

References

[1] [1] Mujumdar As. Handbook of industrial drying. 3rd ed. New York; Marcel Dekker; 2006.

[2] Hazervazifeh A, Nikbakht AM, Maghaddam PA. Novel hybridized drying methods for processing of apple fruit Energy conservation approach. Energy 2016; 103: 679-687.

[3] Sarker MSH, Ibrahim MN, Abdul Aziz N, Punan MS. Energy and exergy analysis of industrial fluidized bed drying of paddy. Energy 2015; 84: 131-138.

[4] Aviara NA, Onuoha LN, Falola OE, Igbeka JC. Energy and exergy analyses of native cassava starch drying in a tray dryer. Energy 2014; 73: 809-817.

[5] Gómez-de la Cruz FJ, Casanova-Peláez PJ, Palomar-Carnicero JM, Cruz-Peragón F. Drying kinetics of olive stone: A valuable source of biomass obtained in the olive oil extraction. Energy 2014; 75: 146-152.

[6] Ranjbaran M, Zare D. Simulation of energetic- and exergetic performance of microwave-assisted fluidized bed drying of soybeans. Energy 2013; 59: 484-493.

[7] Singh S, Kumar S. Solar drying for different test conditions: Proposed framework for estimation of specific energy consumption and CO_2 emissions mitigation. Energy 2013; 51: 27-36.

[8] Culicchi P. L'industria cartaria italiana e il contest europeo. (The Italian paper industry and the european context). Third Workshop Comieco – MIAC (in Italian language) 2002; Lucca (Italy).

[9] Karlsson M., Heikkila P. Computer simulation of yankee drying. Drying ’87 1987; A.S. Mujumdar, Ed. Hemisphere, Washington, 94-202.

[10] Soininen M. A mathematical model for yankee hood. Drying technology 1985; 3: 153-170.

[11] Schukov V, Wozny J. Yankee hood performance studies: the effect of air balance on thermal efficiency. Tappi Journal 1991; 74: 141-145.

[12] Schukov V, Wozny J. Yankee hoods: development of a theoretical model to optimize thermal and electrical efficiency. Tappi Journal 1992; 75: 194-197.

[13] Poirer D, Guadagno J, Tourigny C. Methods of evaluating hood drying rates. Tappi Journal 1996; 79: 183-188.

[14] Onel S, Guruz G. Energy optimization of the yankee-hood dryer. Journal of Mechanical Engineering 2001; 47: 512-518.

[15] Buikis A, Cepitis J, Kalis H, Reinfelds A, Ancitis A, Salmins A. Mathematical models of papermaking. Nonlinear Analysis: Modelling and Control 2001; 6: 9-19.

[16] Yeo Y-K, Hwang K-S, Yi S, Kang H. Modeling of the drying process in paper plants. Korean Journal of Chemical Engineering 2004; 21: 761-766.

[17] Lu T, Shen S Q. Numerical and experimental investigation of paper drying: heat and mass transfer with phase change in porous media. Applied Thermal Engineering 2007; 27: 1248-1258.

[18] Lausijssen J, De Gram F J, Worrell E, Faaij A. Optimizing the energy efficiency of conventional multi-cylinder dryers in the paper industry. Energy 2010; 35: 3738-3750.

[19] Kong L, Liu H. A static energy model of conventional paper drying for multicylinder paper machines. Drying Technology 2012; 30: 276-296.

[20] Chen X, Li J, Liu H, Yin Y, Hong M, Zeng Z. Energy system diagnosis of paper-drying process, Part 1 Energy performance assessment. Drying Technology 2016; 34: 930-943.

[21] Karlsson M. Papermaking Part 2, Drying, IX volume in the Papermaking Science and Technology Series, Tappi.

[22] Bejan A, Kraus A.D. Heat Transfer Handbook 2003. John Wiley & Sons, Inc., Hoboken, USA.

[23] Bird B, Stewart W, Lightfoot E. Transport Phenomena 2002. John Wiley & Sons, Inc., USA.

[24] Martin H. Heat and mass transfer between impinging gas jets and solid surfaces, Academic Press, New York, 1970, 1-60.

[25] Andrew, Hussain. Full coverage impingement heat transfer: the influence of impingement jet size, 1984. First U.K. National Conference on Heat Transfer, Vol. 2: 1115-1124.

[26] Heikkila P., Milosavljevic N. Influence of thermal radiation on the total heat transfer coefficient at high impingement temperatures. NDC'01 - Proceedings of the 1st Nordic Drying Conference, Trondheim, Norway, June 27-29, 2001.

[27] Heikkila P., Milosavljevic N. Investigation of impingement heat transfer coefficient at high temperatures. Drying Technology 2002. Vol. 20: 211–222.

[28] Heikkila P., Milosavljevic N. Influence of Impingement Temperature and Nozzle Geometry on Heat Transfer—Experimental and Theoretical Analysis. Drying Technology 2003. Vol. 21: 1957–1968.

[29] Milosavljevic N., Heikkila P., The wall jet-to surface heat transfer in impingement drying. Drying 2004, Proceedings of the 14th International Drying Symposium, Sao Paulo, Brazil, 22-25 August 2004, Vol. B: 1287-1294.

[30] Lienhard J.H. IV, Lienhard J.H. V, A heat transfer textbook, Phlogiston Press, 2004, USA.

[31] Mill. A., Heat Transfer, CRC Press, 1992.

[32] MATLAB (2012), “MATLAB – The Language of Technical Computing”.

LIST OF FIGURES

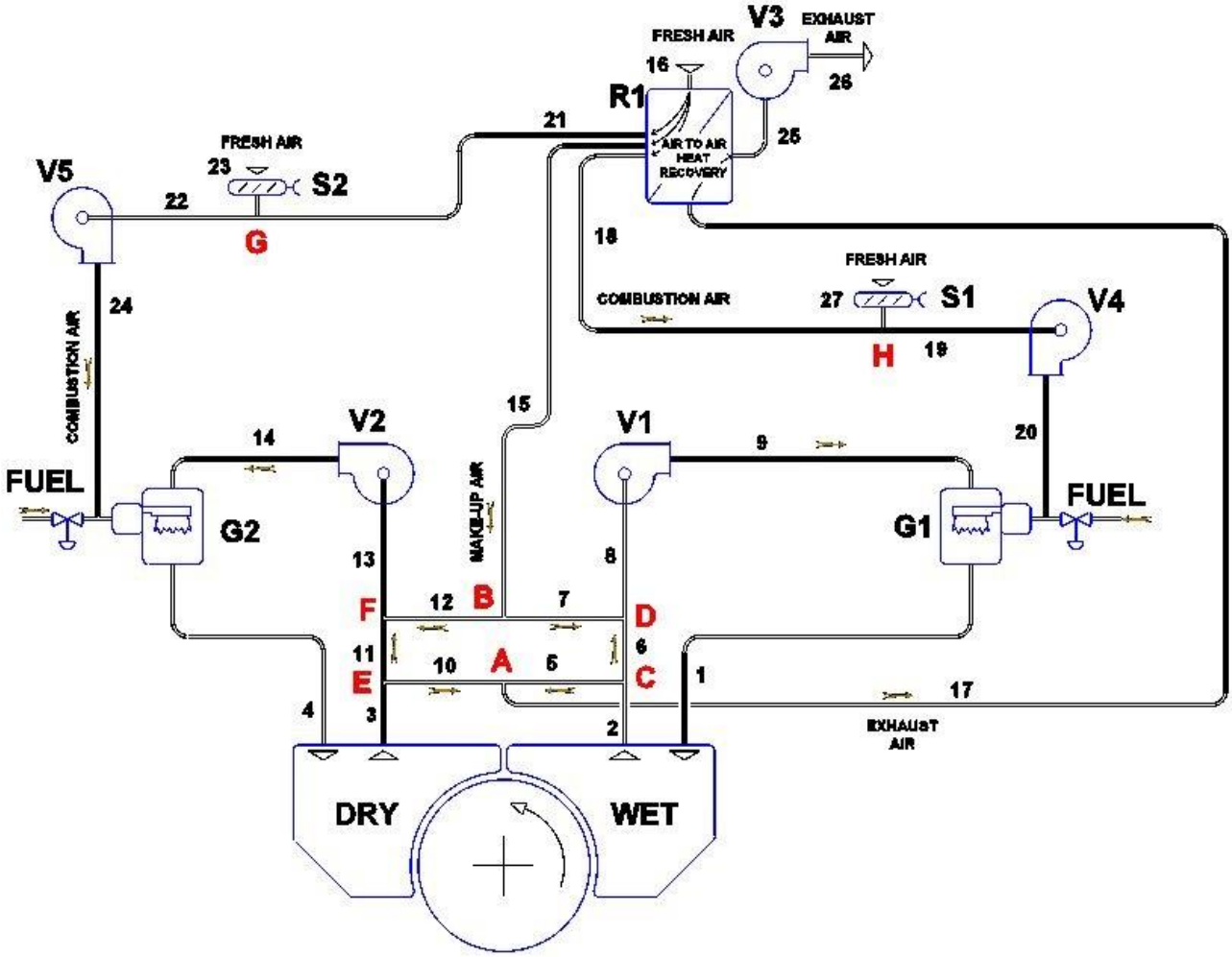

Figure 1. Duosystem configuration with parallel wet–end and dry–end hoods ~~(layout B)~~.

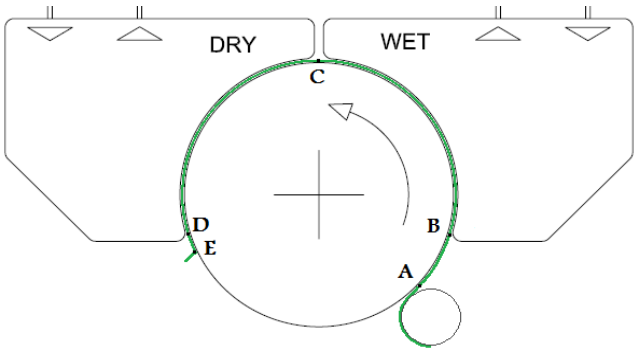

Figure 2. Scheme of the Yankee-cylinder and two air hoods.

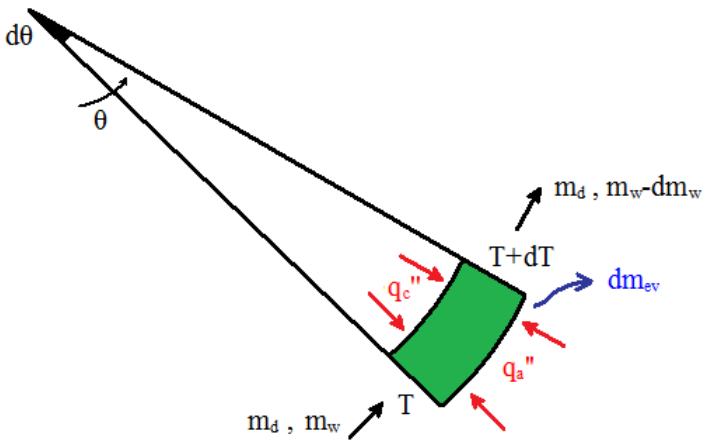

Figure 3. Scheme for the energy balance of the infinitesimal piece of tissue sheet.

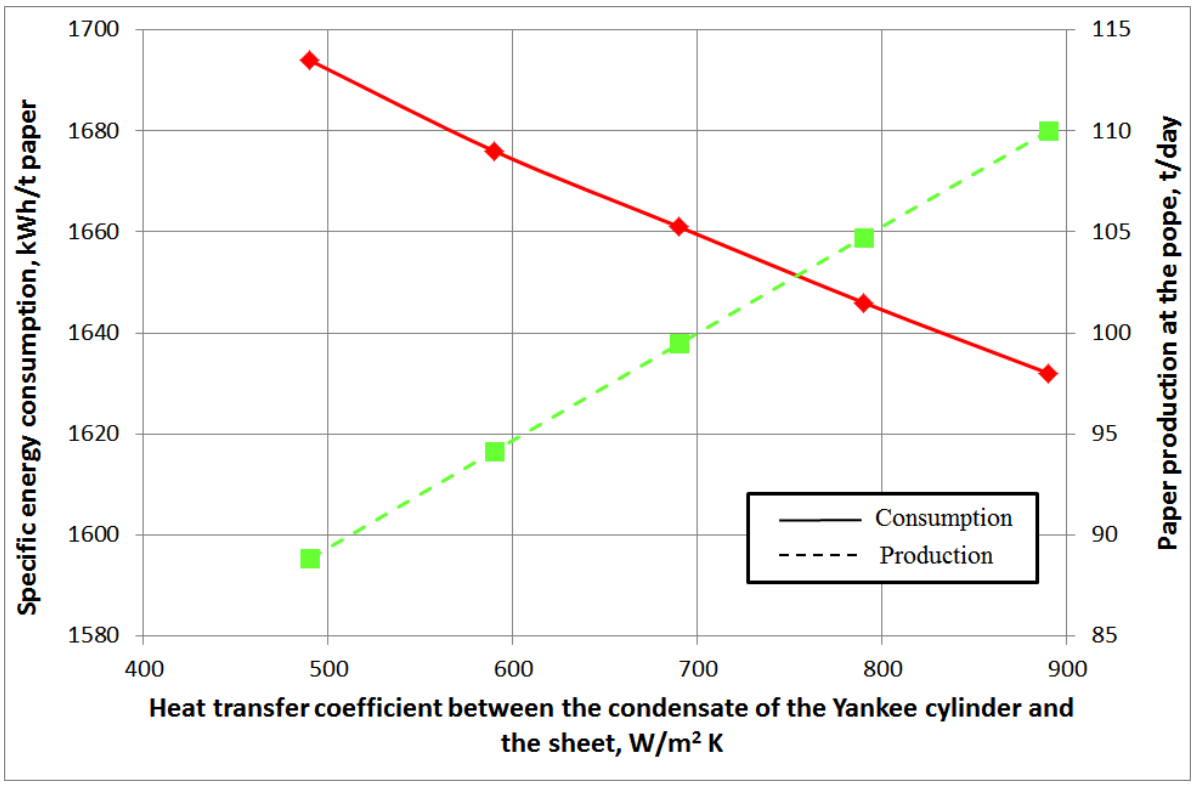

Figure 4. Energy and production performance of the tissue mill in function of the overall heat transfer coefficient of the Yankee cylinder of a duosystem configuration with parallel wet–end e dry–end hoods.

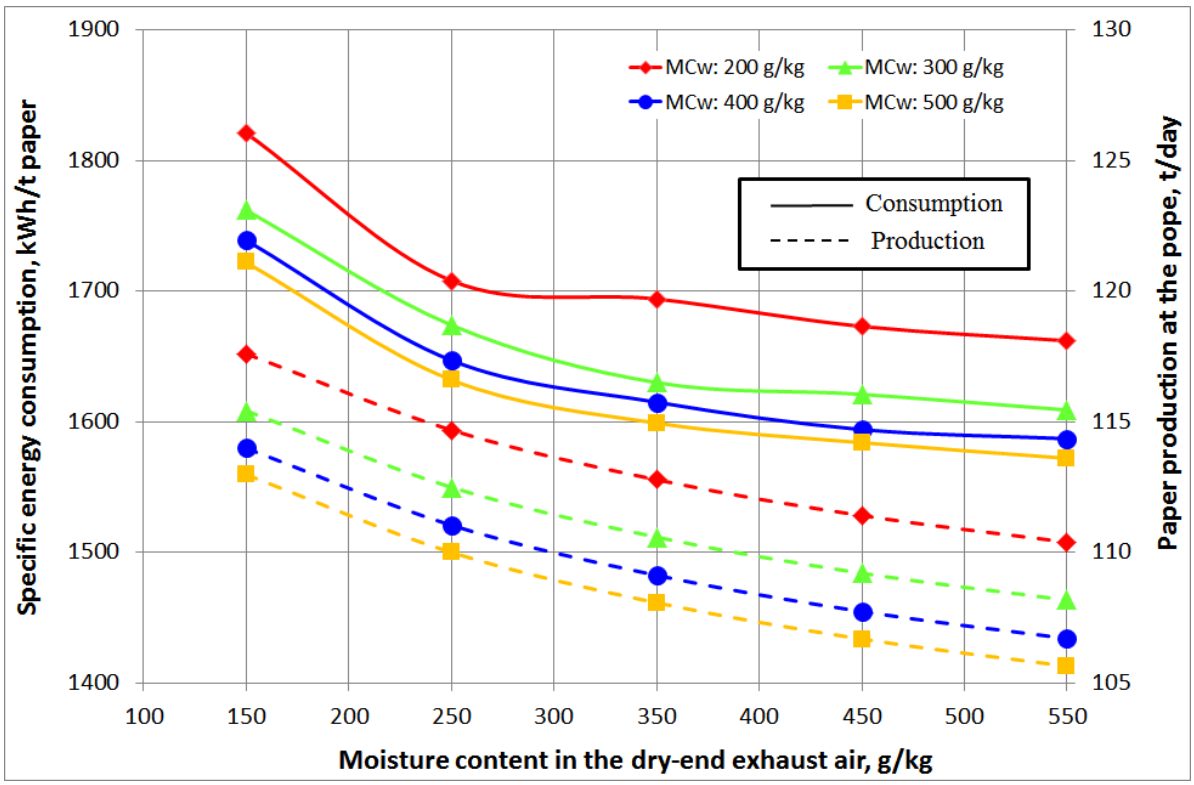

Figure 5. Energy and production performance of the tissue mill in function of the moisture content of the exhaust air of a duosystem configuration with parallel wet–end e dry–end hoods (MCw: moisture content of the wet-end exhaust gas).

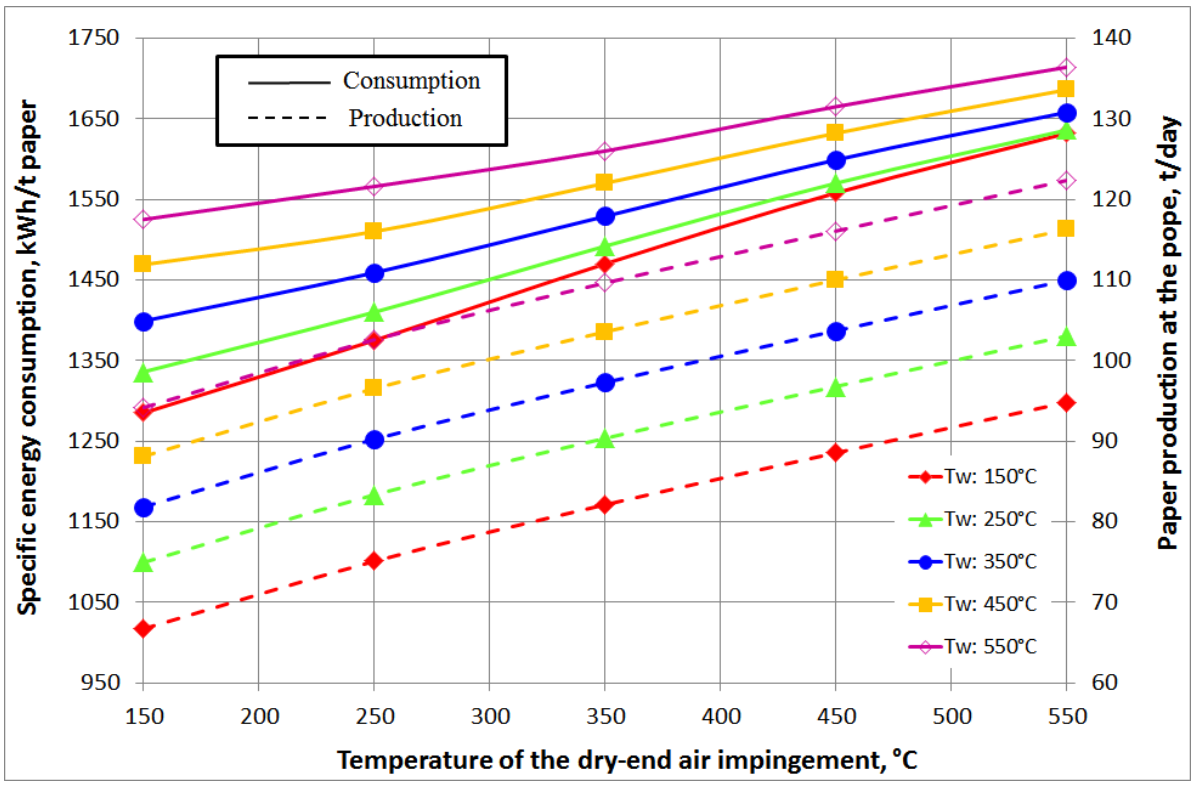

Figure 6. Energy and production performance of the tissue mill in function of the temperature of the air impingements of a duosystem configuration with parallel wet–end e dry–end hoods (Tw: temperature of the wet-end air impingement).

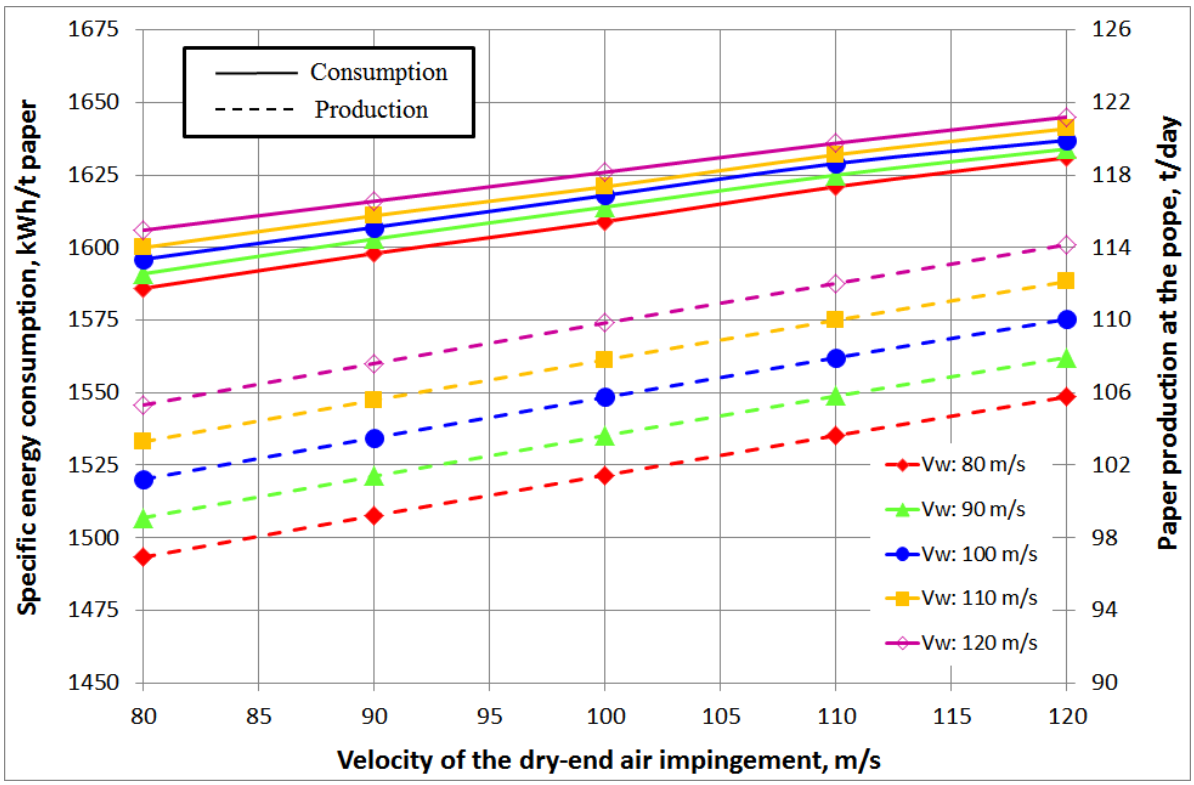

Figure 7. Energy and production performance of the tissue mill in function of the speed of the air impingements of a duosystem configuration with parallel wet–end e dry–end hoods (Vw: velocity of the wet-end air impingement).

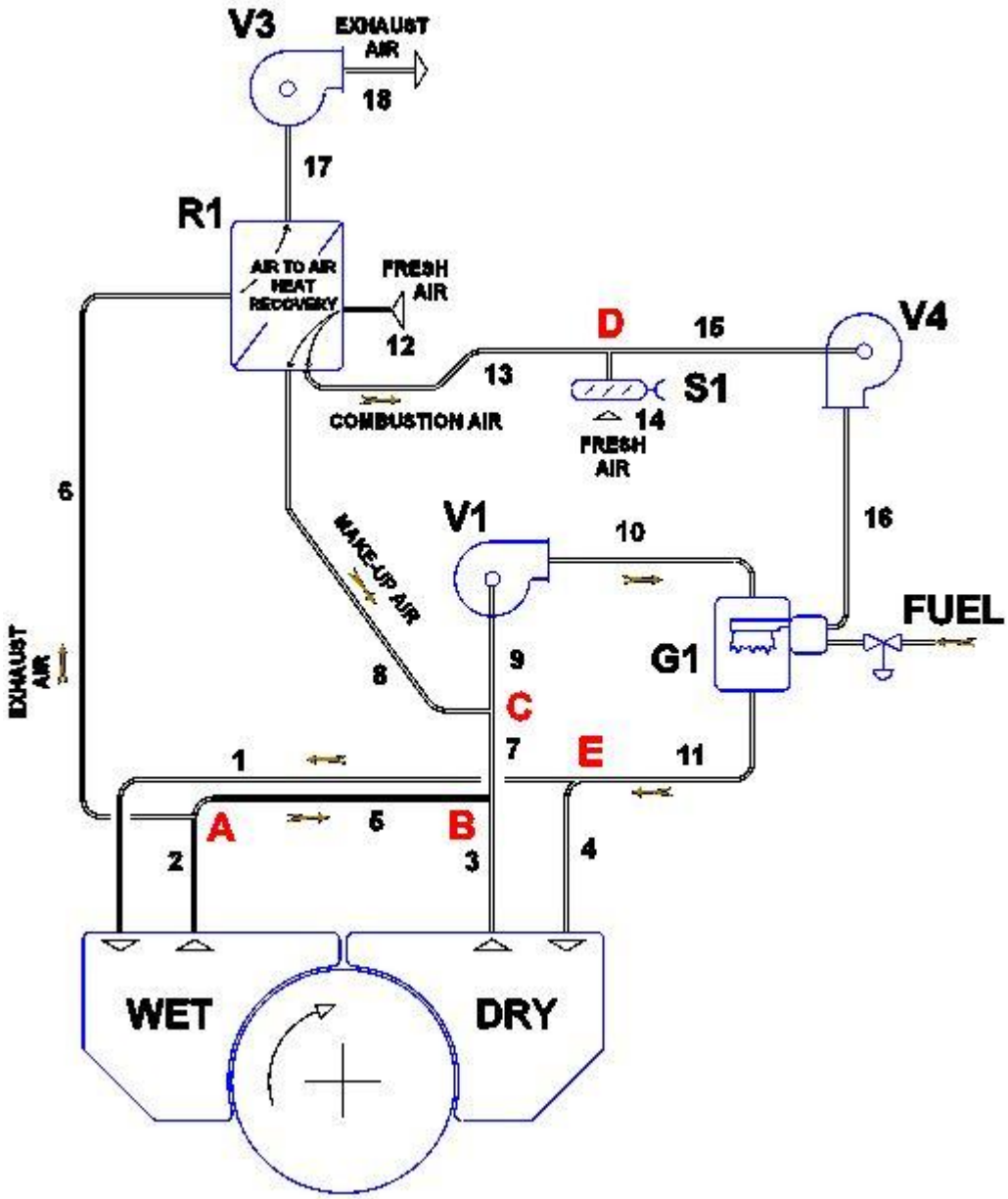

Figure 8. Monosystem configuration.

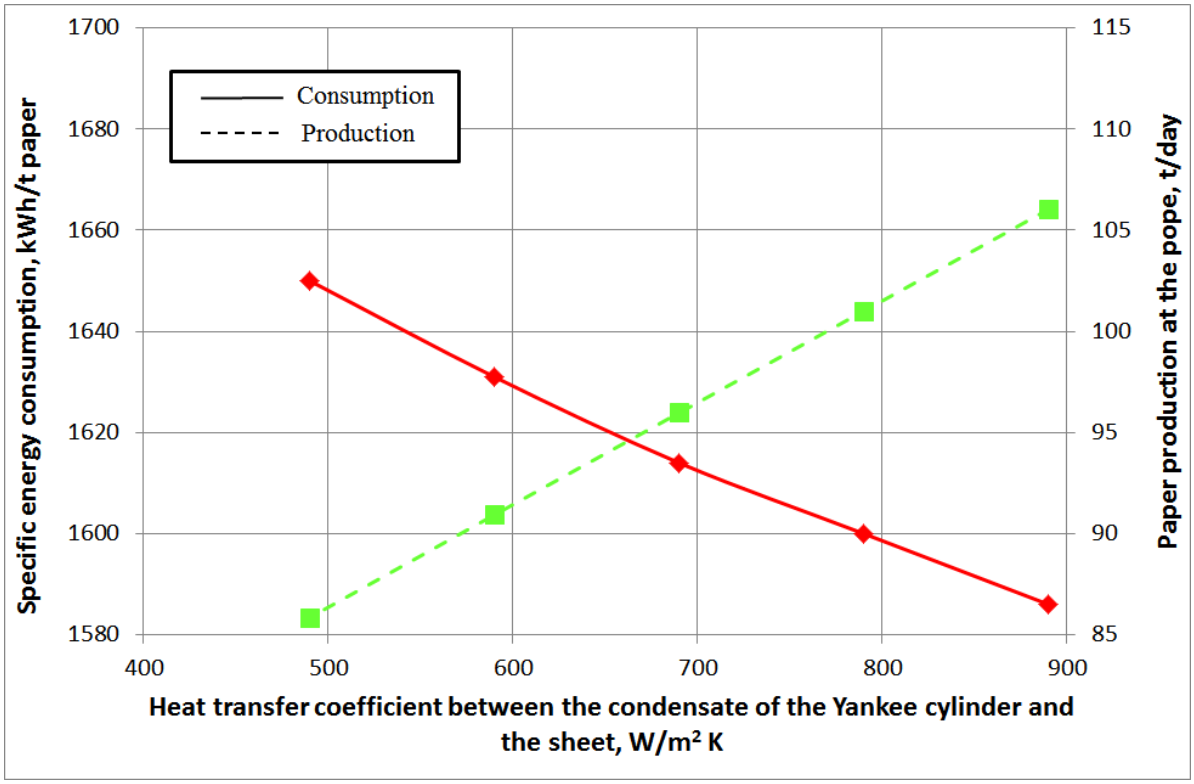

Figure 9. Energy and production performance of the tissue mill with monosystem configuration in function of the overall heat transfer coefficient of the Yankee cylinder.

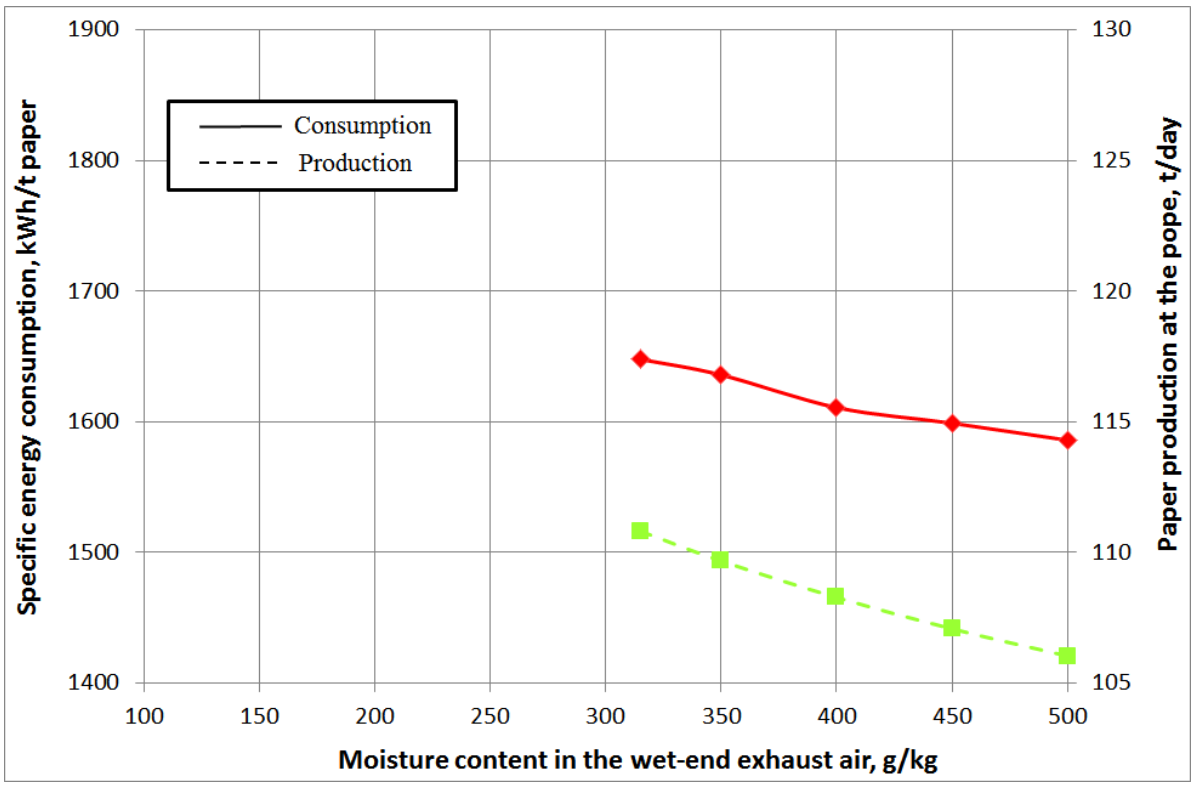

Figure 10. Energy and production performance of the tissue mill with monosystem configuration in function of the moisture content of the exhaust air.

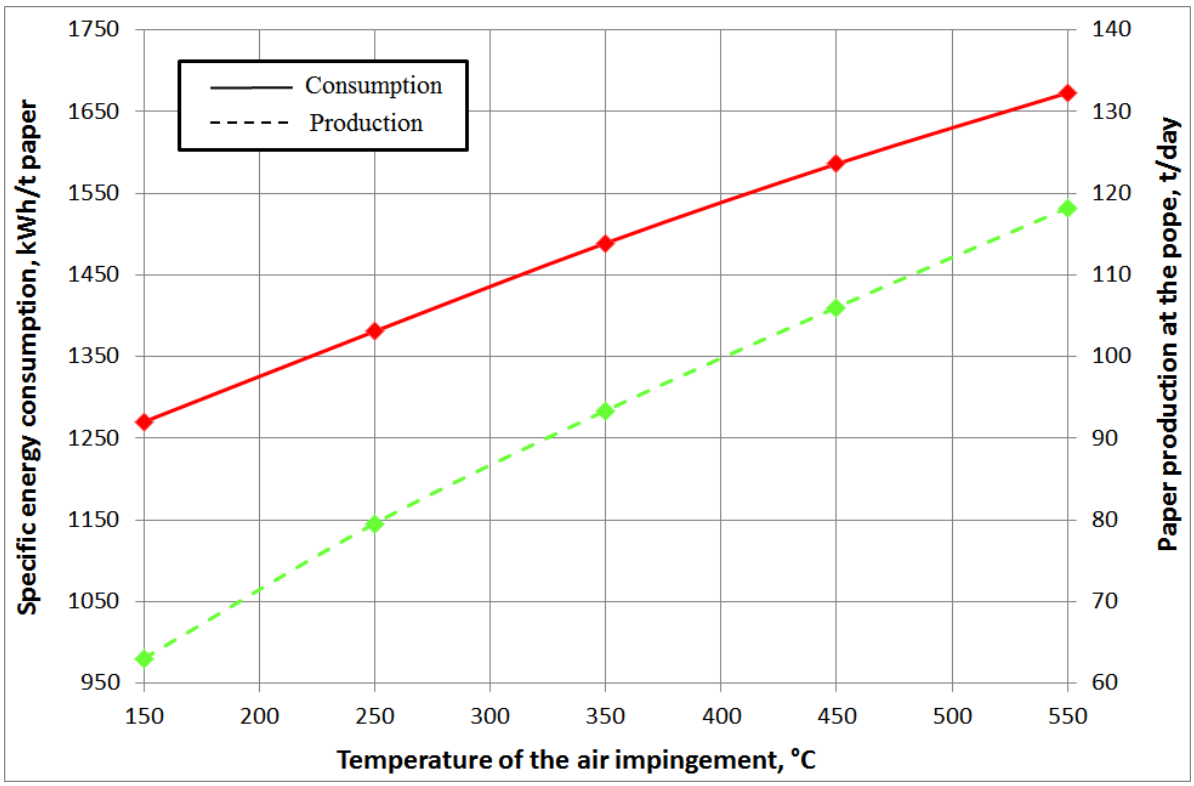

Figure 11. Energy and production performance of the tissue mill with monosystem configuration in function of the temperature of the air impingements.

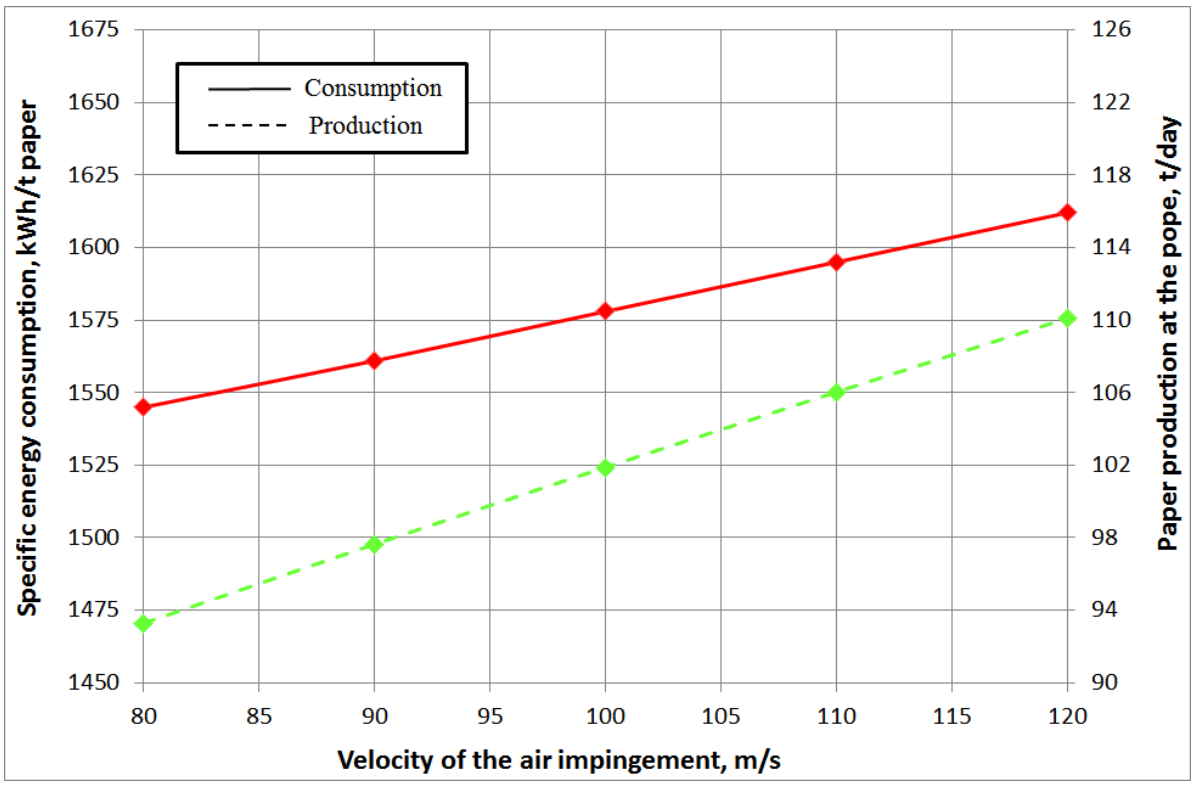

Figure 12. Energy and production performance of the tissue mill with monosystem configuration in function of the speed of the air impingements.

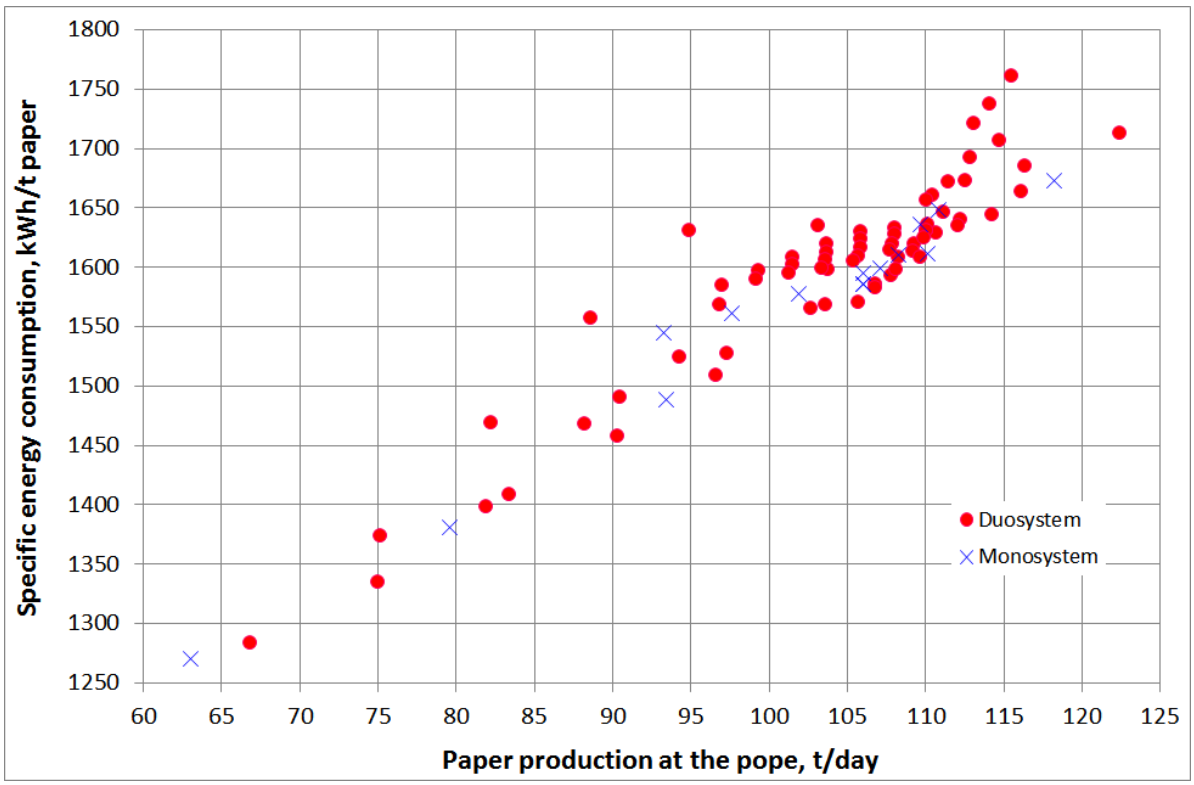

Figure 13. Comparison between the duosystem and monosystem layout.

LIST OF TABLES

Table 1. Input data of the simulation model which are taken from to an existing tissue mill with duosystem configuration and parallel wet–end e dry–end hoods.

INPUTS	
Wrap angle between the press and the inlet of the wet-end hood, °	15
Wrap angle of the wet-end hood, °	125
Wrap angle of the dry-end hood, °	125
Wrap angle between the outlet of the dry-end hood and the doctor blade, °	15
Yankee cylinder diameter, mm	4572
Steam pressure inside the Yankee cylinder, bar	6
Ambient temperature, °C	30
Ambient absolute humidity, g/kg	10
Ambient pressure, bar	1
Air impingement temperature of the wet-end hood, °C	450
Air impingement temperature of the dry-end hood, °C	450
Air impingement speed of the wet-end hood, m/s	110
Air impingement speed of the dry-end hood, m/s	110
Percentage open area of the nozzles within the hoods, -	1.2
Gap between the hoods and the tissue sheet, mm	20
Diameter of the nozzles, mm	5.6
Absolute humidity of the exhaust air from the wet-end hood, g/kg	500
Absolute humidity of the exhaust air from the dry-end hood, g/kg	250
Width of the dried sheet on the Yankee cylinder, mm	2850
Width of the sheet on the pope, mm	2800
Daily production at the pope, t/day	110
Grammage at the pope, g/m^2	18
Coefficient di creping, %	20
Percentage of the in-leaked air within the hoods, -	5
Temperature of the pulp after the vacuum press at the inlet of the Yankee cylinder, °C	38
Heat transfer coefficient of the Yankee cylinder, W/m^2K	890
Fibre content after the vacuum press, %	39
Fibre content at the pope, %	95
Temperature inside the paper mill near the Yankee cylinder, °C	30
Lower heating value of the fuel, MJ/kg	39
Air excess for the burner of the wet-end circuit, %	25
Air excess for the burner of the dry-end circuit, %	25
Maximum allowable temperature of the burner of the wet-end circuit, °C	200
Maximum allowable temperature of the burner of the dry-end circuit, °C	200
Inlet fuel temperature, °C	20

Table 2. Comparison between the results of the simulation model and the real data of an existing tissue mill with duosystem configuration and parallel wet–end e dry–end hoods.

OUTPUTS	Real values	Model values
Overall mass flow of evaporated water, kg/h	6930	6698.9
Specific evaporation rate (referenced to the lateral surface of the Yankee cylinder), kg/m^2 h	76.9	74.1
Thermal power of the drying unit, kW	5305	5126
Steam mass flow of the Yankee cylinder, kg/h	4532	4329.3
Specific energy consumption, kWh/t paper	1610	1632
Specific energy consumption, kWh/t evaporated water	1098	1117
Sheet velocity on the Yankee cylinder, m/min	1823	1818.8
Sheet velocity at the pope, m/min	1519	1515.7
Air impingement mass flow at the wet-end hood, kg/s	7.60	7.25
Air impingement mass flow at the dry-end hood, kg/s	8.20	7.93
Mass flow of the make-up air, kg/s	4.00	3.83
Mass flow of the exhaust air, kg/s	9.00	8.70
Temperature of the exhaust air downstream the wet-end hood, °C	280	275
Temperature of the exhaust air downstream the dry-end hood, °C	259	262
Temperature of the exhaust air, °C	268	266

Table 3. Comparison between the results of the simulation model and the real data of an existing tissue mill with duosystem configuration and parallel wet–end e dry–end hoods.

MCw, g/kg	**MCd, g/kg**	**Specific energy consumption, kWh/t paper**	**Percentage reduction of the specific energy consumption, %**
300	380	1685	-
500	250	1632	3.1
Tw, °C	**Td, °C**	**Specific energy consumption, kWh/t paper**	
350	550	1658	-
550	350	1610	2.9
Vw, m/s	**Vd, m/s**	**Specific energy consumption, kWh/t paper**	
100	120	1637	-
120	100	1626	0.7

Table 4. Results of the simulation model applied to an existing tissue mill with monosystem configuration.

OUTPUTS	
Daily production at the pope, t/day	106.0
Overall mass flow of evaporated water, kg/h	6457.6
Specific evaporation rate (referenced to the lateral surface of the Yankee cylinder), kg/m^2 h	70.1
Thermal power of the drying unit, kW	4977
Steam mass flow of the Yankee cylinder, kg/h	4145.3
Specific energy consumption, kWh/t paper	1586
Specific energy consumption, kWh/t evaporated water	1085
Sheet velocity on the Yankee cylinder, m/min	1753.3
Sheet velocity at the pope, m/min	1461.1
Air impingement mass flow at the wet-end hood, kg/s	7.27
Air impingement mass flow at the dry-end hood, kg/s	7.27
Mass flow of the make-up air, kg/s	1.42
Mass flow of the exhaust air, kg/s	6.1
Temperature of the exhaust air downstream the wet-end hood, °C	275
Temperature of the exhaust air downstream the dry-end hood, °C	275
Temperature of the exhaust air, °C	275